



1 A New Perspective and Explanation to the Formation of  
2 Plasmaspheric Shoulder Structure

3 Hua Zhang<sup>1</sup> Guangshai Peng<sup>1</sup> Chao Shen<sup>2</sup>

4 <sup>1</sup>Institute of Space Weather, Nanjing University of Information Science & Technology,  
5 Nanjing, China.

6 <sup>2</sup>Harbin Institute of Technology, Shen Zhen, China.

7 *Correspondence to:* Hua Zhang (289534957@qq.com)

8 **Abstract**

9 Over the hours of 5-9 UT on June 8 2001, the extreme ultraviolet (EUV) instrument  
10 onboard IMAGE satellite observed a Shoulder-like formation in the morning sector  
11 and a Plume-like structure straddling in the between noon and dusk region.  
12 Simulation results of the plasmopause formation based on mechanism of drift motion  
13 called Test Particle Model (TPM) and have reproduced various plasmopause  
14 structures and subsequent evolution of the Shoulder. The analysis indicated that the  
15 Shoulder is created by a dawn-dusk convection electric field intensity, sharp reduction  
16 and spatial nonuniform manifested. As, combination of the plasmaspheric rotation rate  
17 speed up with L-shell increase and plasma flux do radial outflow in the predawn  
18 sector to interact, and produce an asymmetric bulge that rotates eastward. The  
19 Shoulder-like structure rotates sunward and develops to the single or double Plume  
20 structure during active times.

21 **Keywords:** plasmopause; shoulder-like; plume-like;IMAGE/EUV

22 **1. Introduction**

23 The plasmasphere is important region in the inner magnetosphere, surrounding the  
24 Earth and extending to 5 Earth radii( $R_E$ ), which contains dense( $10$ - $10000\text{ cm}^{-3}$ ) and  
25 cold plasma (below 1eV). The plasmopause formed by a superposition of corotation  
26 and convection electric field in the inner magnetosphere (Nishida,1966; Chen and  
27 Wolf, 1972). The formation and size of plasmopause varies with geomagnetic activity  
28 level. Generally, as the disturbance level increasing, the plasmopause position closer



29 to the Earth and of shape deviate from circle in the equatorial plane (Grebowsky,  
30 1970). Atypical plasmapause structures, such as ‘bulge’ and Plume occur often in both  
31 whistler and in-situ data (Carpenter and Anderson,1992). There are many theoretical  
32 researches study to explanation of the formation of Plume (Grebowsky,1970; Pierrard  
33 and Lemaire, 2004; Zhang et al., 2013).

34 The EUV instrument onboard IMAGE satellite has launched in March, 2000,  
35 which provided a global perspective to the plasmasphere, such as Plume, Finger,  
36 Notch and Shoulder, and so on, some of plasmaspheric structures observed by EUV  
37 (Sandel et al., 2001). One of plasmaspheric structures, Shoulder, has less study in the  
38 previous papers than Plume. But, the Shoulder may play important role on a loss  
39 mechanism for the ring current (Burch et al., 2001). So, it is important to study the  
40 formation mechanism of Shoulder.

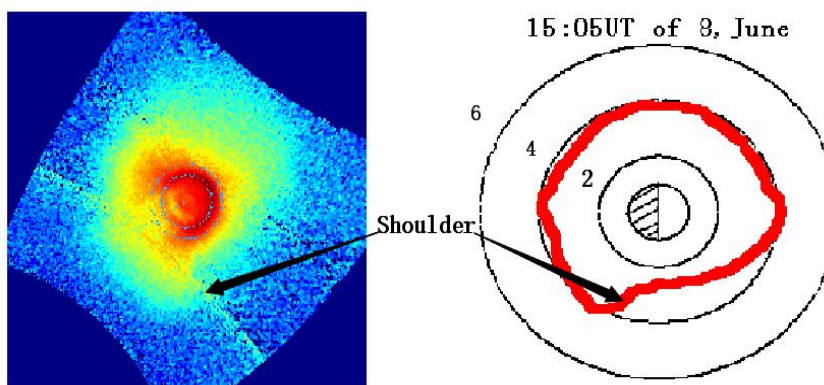
41 At present, there are no convincing explanations for dynamic formation of  
42 Shoulder. Goldstein et al.(2002) firstly proposed an explanation, based on the  
43 Magnetospheric Specification Model(MCM) simulation output, for the formation of  
44 the Shoulder. They presented that the Shoulder is created by sudden decrease of  
45 dusk-dawn electric field. As interplanetary magnetic field (IMF) turns northward  
46 from southward, trigger antisunward flow of plasma in predawn sector, to produce  
47 an asymmetric bulge called Shoulder. Later, based on physical mechanism of  
48 interchange instability and a Kp-dependent E5D electric field model, Pierrard and  
49 Lemaire (2004) suggested that the Shoulder is not the result of radial outflow of  
50 plasma, same as the presentation of Goldstein et al. (2002) , but is inward plasma  
51 drift in post-midnight sector.

52 Then, scarce papers about dynamical formation of the Shoulder are delivered than  
53 of Plume. In this paper, we used TPM to simulate dynamical formation of the  
54 Shoulder, using Weimer’s statistical E-field (Weimer, 2001; Zhang et al., 2012),  
55 which is both spatially nonuniform and dynamically responsive to change  
56 geomagnetic and solar wind conditions. To drive the TPM model, several inputs are  
57 used: Dst; solar wind (SW) and interplanetary magnetic field (IMF) data sets. The  
58 authors make attempt to a new convincing explanation for formation of the



59 Shoulder-like structure, different from the previous explanations.

## 60 2. Shoulder Observation



61  
62 **Figure1. Snapshot of plasmasphere(left panel) by EUV instrument, at 15:05 UT of 8 June 2001,**  
63 **Sunlight is incident from the upper right. Earth is in the center of panels and Shoulder is**  
64 **observed and labeled in the snapshot. Right panel is plasmopause of that extracted from left**  
65 **plasmapheric image.**

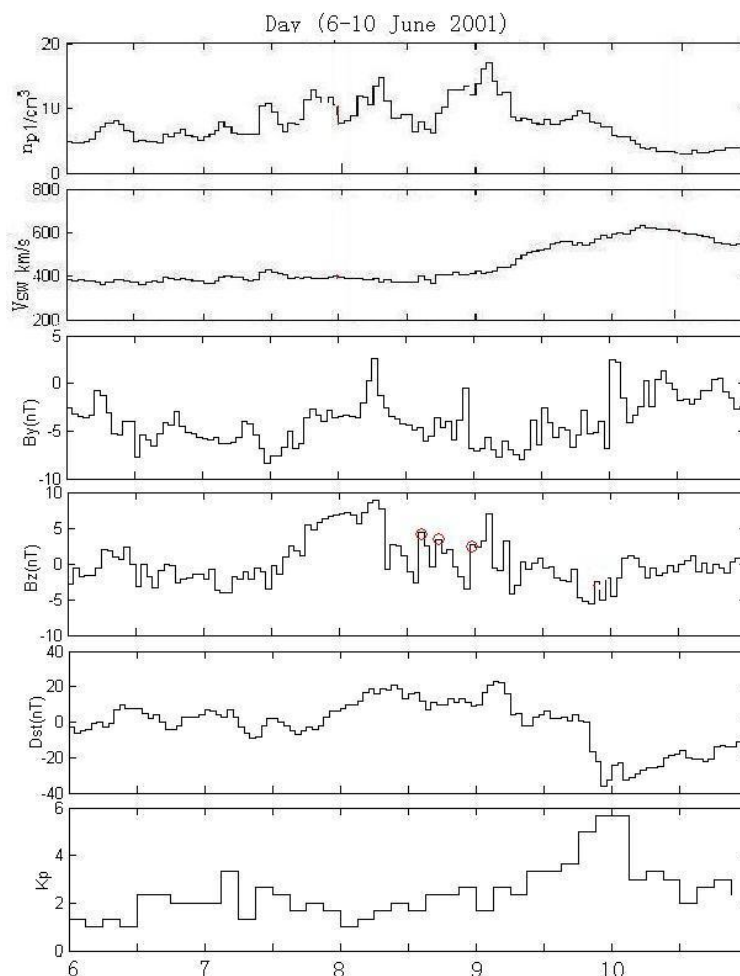
66 The Figure 1 illustrates the Shoulder-like structure, a sharp radial plasmaspheric  
67 structure about 1 RE radial extension, in the post-midnight sector, which was viewed  
68 by EUV imager onboard IMAGE satellite at 15.05 UT of 8 June 2001. The right panel  
69 illustrates the plasmopause extracted from the left panel in the Figure1, and the outer  
70 boundary of plasmasphere is assumed to be 40% of maximum brightness of 30.4nm  
71 He<sup>+</sup> emission, where the intensity is the logarithm of the luminosity (Pierrard and  
72 Cabrera, 2006). Then, the Shoulder-like is labeled and marked by arrows in the plot.  
73 Subsequent pictures show that the Shoulder-like structure remaining and corotating  
74 with main plasmaspheric body by discussion in the next section. That is mean the  
75 outer edge of the Shoulder corotates faster than the inner edge in development phase  
76 (Goldstein et al., 2002). Then, the Shoulder moves eastward to afternoon sector and  
77 evolves into the Plume-like structure. Over the next hours, the outer body of Plume  
78 flows sunward from noon sector, resulting in the Plume thinned out and disappeared  
79 (can see simulation of Figure 3). In the next section, we would discuss simulation of  
80 Shoulder and Plume evolution on 8 June 2001 case base on the TPM method.



### 81 3. Simulation

82 In region of plasmasphere occupied, charged particles are cold plasma (e.g. energy of  
83 particles is several eV or less). So, we can assume that plasma elements have only  $E$   
84  $\times \mathbf{B}/B^2$  drift motions (Li and Xu, 2005; Lejosne and Mozer, 2016). Here, the electric  
85 field intensity of E-model is superposition of convection and corotation electric field.  
86 Electric field plays a key role on plasma drift motion and the formation of  
87 plasmasphere (Pierrard et al., 2008). In the present paper, we use the Weimer's  
88 convection electric field (Weimer, 2001) to model the magnetospheric convection  
89 electric field (Zhang et al., 2012), and T96 magnetic field to model the background  
90 magnetic field.

91 In the simulation, the calculation regions are radial range of 2-7  $R_e$  and azimuthal  
92 span 0-359°. Dispersion by iso-spacing grids that correspond to the radial and  
93 azimuthal steps are equal to 0.1 $R_e$  and 1° respectively, in the magnetic equatorial  
94 plane. Ten particles are placed into each grid, so particle density is proportional to  
95  $L^{-1}$  which is not consistent with the actual density in a saturation state (close to true  
96 density presumably is proportional to  $L^{-3}$ ), but is adequate to study the evolution of  
97 plasmaspheric morphology using a skeleton map of particles during a substorm  
98 period.



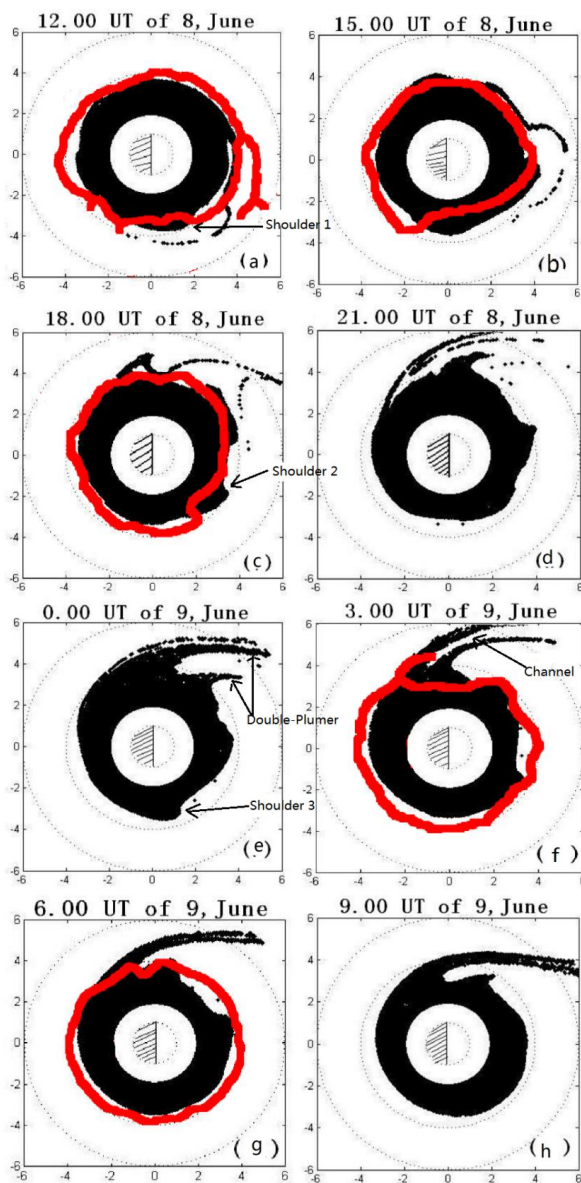
99

100 **Figure 2. Input parameters of TPM model, the variation of the  $B_y$  and  $B_z$  component of the IMF,**  
101 **the Dst index and Kp index, on 6 -10 June 2001, is a typical substorm case.**

102 The paper presents the case of 8-9 June 2001, to study the evolution of the  
103 shoulder and propose a hypothetical explanation produced by TPM simulation.  
104 During the geomagnetic substorm, all of the TPM inputs are available. IMF and Solar  
105 Wind data are available in ACE satellite data center, and Dst index can see in Word  
106 Data center for Geomagnetism, Kyoto. Fig.2 shows the  $B_y$ ,  $B_z$  components of the  
107 IMF, the Dst index and the geomagnetic activity index Kp, observed over 6 to 10 June  
108 2001. This is a typical substorm case that Kp index gradually increases up to 5+ and  
109 then decreases. The TPM run with 3-minute time resolution from 6 June at 00:00 UT



110 to 10 June at 12:00 UT. The results of simulation are showed in Fig.3, which  
111 corresponding times are labeled on the title of each panel. Comparison of TPM  
112 simulation (black body) and EUV observation (red line) in Fig.3, the simulated  
113 plasmopause positions correspond generally rather favorable with the EUV  
114 observations. The results show that the plasmopause is seldom smooth or irregular,  
115 due to the fluctuations in plasmopause region cause by successive particles injection  
116 during a disturbance period (Goldstein et al., 2002; Gallagher et al., 2005), verified by  
117 simulation and EUV observation, in agreement with previous whistler observations  
118 (Carpenter and Anderson,1992). In addition, observations and simulations are not  
119 identical, due to deviation in the extraction of the boundary from EUV image and  
120 optical contamination of the image (Sandel et al., 2001; Zhang et al., 2013).



121

122 **Figure 3.** The simulation of plasmaspheric morphology compare with EUV/IMAGE observation in the  
123 geomagnetic equatorial plane on 8 - 9 June 2001. The red irregular curves indicate the plasmapause  
124 observation by EUV. The dotted circles on the panels correspond to L=1, 2, 4 and 6.

125 Panels of Fig.3(a) - (h) illustrate the plasmasphere obtained on the interval of from  
126 8 June at 12:00 UT to 9 June at 09:00 UT 2001, and every three hours output a



127 snapshot. The results of the simulation show that the evolution and development of  
128 the features of the plasmopause, like Shoulders and Plumes. One can see that the  
129 plasmopause is sharper and becomes closer to the Earth in the predawn sector. The  
130 reason is the increase of rotation velocity resulting in plasmopause of peeled off in the  
131 predawn sector (Pierrard and Cabrera, 2006; Verbanac et al., 2018). At 15.05 UT of 8  
132 June, the TPM simulation captures a infant Shoulder-like structure in panel Fig.3 (b),  
133 and then corotates with the plasmasphere body moved eastward and further  
134 reproduces a mature Shoulder formation in Fig.3(c). The overall agreement between  
135 TPM simulation and EUV observed is quite well, but the TPM Shoulder is located  
136 ~1.5 hours earlier in magnetic local time (MLT) that probably originated from the  
137 convection electric field model (Goldstein et al., 2002; Pierrard and Cabrera, 2005 ;  
138 Zhang et al., 2013).

139 The EUV observation illustrated in Fig.3 (f) shows that a Plume is indeed observed  
140 in the afternoon or dusk sector. The results of the simulation also reproduce the  
141 formation and the motion of the Plumes, which derive from the Shoulder structure,  
142 illustrated in panels of Fig.3 (d)-(f). The simulation show that the Shoulders generate  
143 in the post-midnight sector (Verbanac et al., 2018), and then rotates eastward around  
144 the Earth to the afternoon sector (Goldstein et al., 2002). When the level of  
145 geomagnetic activity increase, the plasma element in the Shoulder around the outer  
146 plasmasphere would convection outward and then into the dayside magnetopause (Li  
147 and Xu, 2005; Pierrard et al., 2008), and produce the plasmaspheric Plume structure.  
148 The Shoulder1 firstly arises at 12 UT in the morning sector( see in Fig.3(a)), and then  
149 corotates with the Earth reaching to the afternoon region at 18 UT ( see in Fig.3(c)),  
150 on 8 June 2001. At this time, Kp index increases to 3+ ( see in Fig.2), and  
151 magnetosphere convection slightly enhance that trigger plasma elements in the  
152 Shoulder1 doing sunward convection, then produce the Plumel at 21 UT on 8 June  
153 2001 (see in Fig.3(d)). The mature Shoulder2, illustrated in Fig.3(b), corotates  
154 eastward with the Earth to the afternoon-dusk sector. During period of 0-3 UT on June  
155 9, Kp index gradually increases up to 5+, indicating that magnetospheric convection  
156 is enhanced and the convective electric field increases. The infantile Plume2,





157 illustrated in the panel of Fig.3(e), derives from outflow of plasma elements in the  
158 Shoulder2, and evolves into the mature Plume2 in Fig.3(f). Later, the double-plumes  
159 formation that is extension from the plasmopause to the magnetosphere, presented in  
160 the simulation results in panels of Figs.3 (e)-(f).

161 The cavity in between the double Plumes, or between Plumes and the main body  
162 of plasmasphere, may be responsible for the formation of Channel and Notch  
163 structures (Gallagher et al., 2005). The base and the westward edge of the Plume is  
164 connected with the main body of plasmasphere. And there is a cavity topology, a  
165 low-density region, between the tail structure of the plasmasphere and the main body  
166 of plasmasphere. That is the channel structure of the plasmasphere. The Plume  
167 corotates with the Earth to become thinner, and disappear finally (Li and Xu, 2005).  
168 The plasma refilling from plasma sheet results in the Notch structure disappear  
169 (Gallagher et al., 2005). The results of simulation show the Channel structure in  
170 Fig.3(e)-(f). Gallagher et al. (2005) proposes that Notches and Channels share same  
171 origin, which derive from a low-density cavity in the dusk region during recovery at  
172 the base of the plasmaspheric Plume. The absence of Notch structure in this  
173 simulation event, due to the fact that the potential structure does not cause the inward  
174 convection of plasma in the afternoon sector, and the low disturbance time is  
175 maintained for no long enough time.

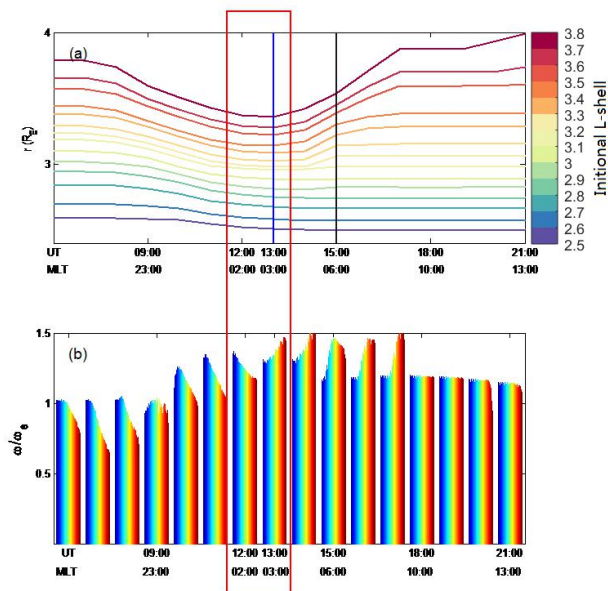
176 By contrastive analysis on between Fig.2 and Fig.3, the formation of the  
177 Shoulder is produced during the intensity of the convection electric field sudden  
178 decrease (Goldstein et al., 2002; Pierrard and Lemaire, 2004), when IMF turns  
179 northward. There are three Shoulders produced during this substorm period, depicted  
180 in panels of Fig.3 (b)-(g). The time of the Shoulder appearance are labeled by three  
181 red circles in Fig.2, at 14:00 UT, 17:00 UT, 23:00 UT on 8 June respectively. At  
182 moment, the Bz component of the IMF turns northward. But, not all of the times as  
183 the Bz component of the IMF turns northward, could produce the Shoulder structure.  
184 The Bz value must lower than previous 24-hours value, due to the intensity of the  
185 convection electric field lower than previous level, so the last closed equipotential line  
186 (LCE) would close to the Earth and result in plasmopause of peeled off in the



187 predawn sector (Zhang et al., 2013). One can see that no shoulder appearance in the  
188 results of the simulation, produced at 02:00 UT, 05:00 UT, and 08:00 UT on 9 June  
189 2001 respectively.

#### 190 4. Discussion

191 The physical explanation of Shoulder formation is not yet understood. In present  
192 section, we use the case of Fig.1 as an example to investigate the physical mechanism  
193 of Shoulder formation based on the TPM model. Fourteen test particles are placed in  
194 the range of  $2.5 \leq L \leq 3.8$ , initial position locate at 12:00 MLT, space step takes  $0.1R_e$ ,  
195 and then trace these particles motion. Outputs are the trajectory (see in Fig.4(a)) and  
196 the rotation rate (see in Fig.4(b)) of these test particles corresponding to given  
197 magnetic local time and universal time illustrated in the bottom of Fig.4.



198  
199 **Figure 4.** The trajectory (upper plot) and the rotation rate (bottom plot) of 14 test particles  
200 corresponding to given magnetic local time and universal time during a substorm, to explain the  
201 physical mechanism of Shoulder formation. Fourteen test particles are placed in the range of  
202  $2.5 \leq L \leq 3.8$ , initial position locate at 12:00 MLT, and space step takes  $0.1R_e$   
203



204 The top panel shows that the outer part of plasmasphere ( $L > 3.3$  Re) drift inward in  
205 the before 02:00 MLT sector, and move outward (could reach up to 3.9 Re position) in  
206 the predawn sector (after 03:00 MLT sector) (Verbanac et al., 2018). The radial motion  
207 of inner plasmasphere ( $L < 3.3$ ) is negligible. So, the Shoulder has a sharp eastern edge  
208 about  $0.5R_e \sim 0.7R_e$  in radial extension and in a range of 3 MLT. Goldstein et al. (2002)  
209 proposed the shoulder formation by an outward radial motion of plasma in a narrow  
210 range and in the morning sector. The conclusions of Goldstein (2002) and Verbanac  
211 (2018) verify the simulation of this paper.

212 The lower panel shows the corotational angular velocity of test particles in the  
213 range of  $2.5 < L < 4.0$ . The simulation results suggest that plasma element in  
214 plasmasphere region rotation speed varies significantly with radial distance (Galvan,  
215 2010). The inner part of plasmasphere rotates faster than its outer part in before 02:00  
216 MLT sector, vice versa in a range of in the 03:00-08:00 MLT sector [Lejosne and  
217 Mozer, 2016]. The previous researchers analyze the EUV observation and propose the  
218 Shoulders structure have MLT sharpening in the angular direction, which indicate the  
219 outer edge of the Shoulder rotates faster than the inner edge, resulting in the gradual  
220 increase of MLT-profile of the Shoulder (Goldstein et al., 2002). The lower panel  
221 shows, with the increase of  $L$ , the rotation rate of the plasmasphere tends to slightly  
222 decrease on the dusk side and obviously increase on the dawn side.

223 Fig. 4 indicate, in the region of 21:00 - 23:00:00 MLT, that the rotation rate is  
224 about corotation in the inner plasmasphere ( $L < 3$ ), but is the interval of 70% - 90% of  
225 corotation in the outer plasmasphere ( $L > 3$ ). The rotational value decreases with the  
226 increase of  $L$  [Galvan et al., 2010]. Gallagher et al. (2005) investigates the drift rate of  
227 notches in the geomagnetic quiet phase, and the results show that the average rotation  
228 rate of plasmasphere is about 90% of the corotational rate, in agreement with the  
229 results of Lejosne and Mozer (2016). When the plasma elements rotate to the region  
230 of 23:00 - 02:00 MLT, rotation rate in the outer plasmasphere reaches to  $\sim 130\%$  of  
231 corotation, and in the inner plasmasphere is also close to the corotation rate. The  
232 results show that the rotation rate of plasmasphere is overall increasing in the region.  
233 When the plasma elements rotate into the region of between 03:00 and 08:00 MLT,



234 the plasma elements in the outer plasmasphere move outward and have a radial  
235 outflow of about the interval of 0.2 - 0.7 Re. In addition, the plasma elements in the  
236 outer plasmasphere rotate faster than the inner plasmasphere in this region. The  
237 Fig.4(b) shows that rotation rate in the outer plasmasphere highly reaches to ~ 140%  
238 of corotation, and rotation rate in the inner plasmasphere is close to 110% of  
239 corotation. So, we suggest that the physical mechanism of shoulder formation is the  
240 result of plasma extrusion in the predawn sector, caused by outer plasmasphere drifts  
241 radial outward and rotates faster. In present paper, the results show that the rotation  
242 rates of simulation are higher than the observations, and not consistence with Huang  
243 et al. (2011) and Galvan et al. (2010). The first reason is that the level of Kp index and  
244 the convection of magnetosphere is increase, so the value of these parameters driven  
245 convection field in this case is greater than the previous study articles in the  
246 geomagnetic quite case (Galvan et al., 2010; Huang et al., 2011 ; Verbanac et al.,  
247 2018 ). And the second reason is that the model does not include the shielded electric  
248 field, which results in a larger total electric field value in calculation (Goldstein et al.,  
249 2002; Pierrard et al., 2008).

250 The dawn-dusk asymmetry of convective electric field is caused by the terminal  
251 conductivity gradient of the ionosphere. The subrotation of the ionosphere drives the  
252 subrotation of the plasmasphere, and the plasmaspheric drift is correlated with the  
253 phase of geomagnetic storm (Burch et al., 2004). The convection electric field of  
254 Weimer (2001) is obvious dawn-dusk asymmetry, that causes a smaller increase on  
255 the downside and a lager decrease on the duskside, indicating that the subrotational  
256 effect of the plasmasphere is modulated by field-aligned current changes and  
257 conductance variations (Liemohn et al., 2004). The asymmetry of potential pattern  
258 causes the sunward convection in the magnetospheric night-side to be larger than that  
259 in the morning side, resulting in the subcorotational flow in the dark side and the  
260 supercorotational flow in the morning side (Gallagher et al., 2005).

261

## 262 5. Conclusion



263 In this paper, we have simulated the case of substorm on 8 June 2001 to investigate  
264 the physical mechanism of Shoulder formation based on TPM model that utilizes  
265 Weimer's electric field and the drift motion theory. We use the E-model and the  
266 B-model are quasi-static background field and global averages. So, the results of  
267 simulation have some deviations with EUV observation. But, we have satisfactorily  
268 reproduced the evolution and development of the features of the plasmopause, like  
269 Shoulders and Plumes. And then, the physical mechanism of Shoulder formation has  
270 been investigated. The following results are obtained:

271 1. The formation of Shoulder is association with IMF northward turning in the  
272 predawn sector. But not all of IMF northward turning could produce shoulders. It  
273 is only that  $B_z$  of IMF value must lower than previous 24 hours value.

274 2. The physical mechanism of Shoulder formation is the result of plasma extrusion  
275 in the predawn sector, caused by outer plasmasphere drifts radial outward and  
276 rotates faster.

277 3. The formation and evolution of Plumes have also been study in this paper. One  
278 can see single or double Plumes appear in the dusk or afternoon sector, and then  
279 become thinner with time, finally disappear. A second-Plume derives from the  
280 Shoulder which rotates to the afternoon sector and convects into the outer  
281 magnetosphere and then forms the second-Plume.

282 At this model, we not consider the refilling process of ionosphere. In the future  
283 work, the refilling process should be considered, expect to obtain more perfect results  
284 comparing with EUV observations. And also, the physical mechanisms of  
285 plasmaspheric features observed by EUV/IMAGE, like Notch or Channel, also are to  
286 investigate by TPM model in future work underway.

287 **Author contributions:** Zhang H. conceptualized the project and wrote the original  
288 draft of the paper. Peng G. S. modified the Figures and coded Fortran program. Shen C.  
289 supervised the project, and reviewed and edited the paper.

290

291 **Acknowledgment:** The author thanks the professor D. R. Weimer, who provided the  
292 code of Weimer's electric field model and ACE satellite data center and Word Data



293 center for Geomagnetism, Kyoto provided observation data. The dataset of  
294 EUV/IMAGE could download from website <http://euv.lpl.arizona.edu/euv>.

295

## 296 **References**

297 Burch, J. L., Mende, S. B., Mitchell, D. G., Moore, T. E. , Pollock, C. J., Reinisch, B.  
298 W., Sandel, B. R., Fuselier, S. A. , and Gallagher D. L.: Views of Earth's  
299 magnetosphere with the IMAGE satellite, *Science*, 291, 691-624, doi:  
300 10.1126/science.291.5504.619, 2001.

301 Carpenter, D. L. and Anderson, R. R.: An ISEE/Whistler model of equatorial  
302 electron density in the magnetosphere, *J. Geophys. Res.*, 97, 1097-1108,  
303 doi:10.1029/91JA015481992, 1992.

304 Chen, A. J. and Wolf, R.A. : Effects on the plasmasphere of a time-varying convection  
305 electric field, *Planet. Space Sci.*, 20, 483-509, doi: 10.1016/0032-0633(72)90080-3,  
306 1972.

307 Gallagher, D. L., Adrian, M. L. and Liemohn, M. W.: Origin and evolution of deep  
308 plasmaspheric notches, *J. Geophys. Res.*, 110, A09201, doi:10.1029/2004JA010906,  
309 2005.

310 Galvan, D. A., Moldwin, M. B., Sandel, B. R., and Crowley, G. : On the cause of  
311 plasmaspheric rotation variability: IMAGE EUV observation, *J. Geophys. Res.*, 115,  
312 A01214, doi:10.1029/2009JA014321, 2010.

313 Goldstein, J., Spiro, R. W., Reiff, P. H., Wolf, R. A., Sandel, B. R., Freeman, J. W., and  
314 Lambour, R. L.: IMF-driven overshielding electric field and the origin of the  
315 plasmaspheric shoulder of May 24, 2000, *Geophys. Res. Lett.*, 29(16), 1819,  
316 doi:10.1029/2001GL014534, 2002.

317 Grebowsky, J. M.: Model study of plasmopause motion, *J. Geophys. Res.*, 75,  
318 4329-4333, doi:10.1029/JA075i022p04329, 1970.

319 Huang Y., Xu, R. L., Shen, C., and Zhao H.: Rotation of the Earth's plasmasphere at  
320 different radial distances, *Adv. Space. Res.*, 48, 1167-1171, doi:  
321 10.1016/j.asr.2011.05.028, 2011.

322 Lejosne, S., and Mozer, F. S. : Van Allen Probe measurements of the electric drift



- 323  $E \times B/B^2$  at Arecibo's L=1.4 field line coordinate, *Geophys. Res. Lett.*, 43, 6768-6774,  
324 doi: 10.1002/2016GL069875, 2016.
- 325 Li, L., and Xu, R. L.: Model of the evolution of the plasmasphere during a  
326 geomagnetic storm, *Adv. Space. Res.*, 36, 1895-1899. doi: 10.1016/j.asr.2003.10.057,  
327 2005.
- 328 Nishida A.: Formation of plasmopause, or magnetospheric plasma knee, by the  
329 combined action of magnetospheric convection and plasma escape from the tail, *J.*  
330 *Geophys. Res.*, 71, 5669-5679, doi:10.1029/JZ071i023p05669, 1966.
- 331 Pierrard V., and Lemaire, J. F.: Development of shoulders and plumes in the frame of  
332 the interchange instability mechanism for plasmopause formation, *Geophys. Res. Lett.*,  
333 31, L05809, doi:10.1029/2003GL018919, 2004.
- 334 Pierrard, V., and Cabrera, J.: Comparisons between EUV/IMAGE observations and  
335 numerical simulations of the plasmopause formation, *Annales Geophysicae*, 23,  
336 2635-2646, doi:10.5194/angeo-23-2635-2005, 2005.
- 337 Pierrard, V., and Cabrera, J.: Dynamical simulations of plasmopause deformations,  
338 *Space.Sci.Res*, 122, 119-126, doi: 10.1007/s11214-006-5670-3, 2006.
- 339 Pierrard, V., Khazanov, G. V., Cebreira, J., and Lemaire, J.: Influence of the convection  
340 electric field models on predicted plasmopause positions during magnetic storms. *J.*  
341 *Geophys. Res.* 113, A08212, doi:10.1029/2007JA012612, 2008.
- 342 Sandel, B. R., King, R. A., Forrester, W. T., Gallagher, D. L., Broadfoot, A. L., and  
343 Curtis, C. C.: Initial results from the IMAGE extreme ultraviolet imager, *Geophys.*  
344 *Res. Lett.*, 28, 1439, doi: 10.1029/2001GL012885, 2001.
- 345 Verbanac, G., Bandic, M., Pierrard, V., and Cho, J.: MLT plasmopause characteristics:  
346 Comparison between THEMIS observations and numerical simulations. *J. Geophys.*  
347 *Res: Space physics*, 123, 2000-2007, doi:10.1002/2017JA024573, 2018.
- 348 Weimer, D. R.: An improved model of ionospheric electric potentials including  
349 substorm perturbations and application to the Geospace Environment Modeling  
350 November 24, 1996, event., *J. Geophys. Res.*, 106, 407-416,  
351 doi:10.1029/2000JA000604, 2001.
- 352 Zhang, H., Xu, R. L., Zhao, H., and Shen, C.: The characteristics of the model of



353 Weimer's electric field within the magnetosphere., Chinese J. Geophys. 55, 36-45, doi:  
354 10.6038/j.isnn.0001-5733.2012.01.004, 2012.  
355 Zhang, H., Xu, R. L., Shen, C., and Zhao, H.: The simulation of the plasmaspheric  
356 morphology during a magnetospheric disturbance event, Chin J. Geophys, 56,  
357 731-737, doi:10.6038/cjg 20130302, 2013.